THE JOURNAL OF PHYSICAL CHEMISTRY B

Article

pubs.acs.org/JPCB

Dilational Properties of Novel Amphiphilic Dendrimers at Water−Air and Water−Heptane Interfaces

Pei Zhang,[†] Lei Zhang,[‡] Lu Zhang,[‡] Jizhu Zhou,[†] Jinben Wang,*[,†] and Haike Yan[†]

[†]Beijing National Laboratory for Molecular Sciences, Key Laboratory of Colloid, Interface and Chemical Thermodynamics, Institute of Chemistry, Chinese Academy of Sciences, Beijing 100190, P. R. China

[‡]Technical Institute of Physics and Chemistry, Chinese Academy of Sciences, Beijing 100190, P. R. China

Supporting Information

ABSTRACT: In this work, a series of novel amphiphilic dendrimers taking polyamidoamine dendrimer as the core with different hydrophobic tails $QPAMC_m$ were synthesized and the dilational properties were studied as monolayers by dilational rheological measurements at the water−air and water−*n*-heptane interfaces to explore the nature of adsorption behaviors. The results showed that the maximum values of the dilational modulus seemed to have no obvious variation in a wide change of hydrophobic chain length at the surface. However, there was considerable variability in the tendency of the influence of bulk concentration on the dilational modulus at the two different interfaces. It was interestingly found that the diffusion-exchange process slowed down with the increase of alkyl chain length leading to more elastic nature of adsorption film, which was contrary to the tendencies of conventional single chain and gemini surfactants. It is reasonable to consider that, in the case of the molecule having short chain length such as $QPAMC_8$, the alkyl chains are too short to overlap across the headgroup, enable the intermolecular hydrophobic interaction to be predominant with increasing of surface concentration, which enhances the elasticity and shows the slowest diffusion-exchange process. Whereas, when the chain length increases to 12 or 16, the alkyl chains are long enough to act intramolecularly to form intracohesion conformation, which results in enhancing the diffusion-exchange process. In conclusion, the interfacial behaviors are dictated by the size ratio between the tail and headgroup. A reasonable model with respect to the molecular interaction was proposed on the basis of experimental data. The results of interfacial tension relaxation and dynamic light scattering (DLS) experiments, in accord with the proposed mechanism, also present the unusual tendency comparing to the traditional single or gemini surfactants.

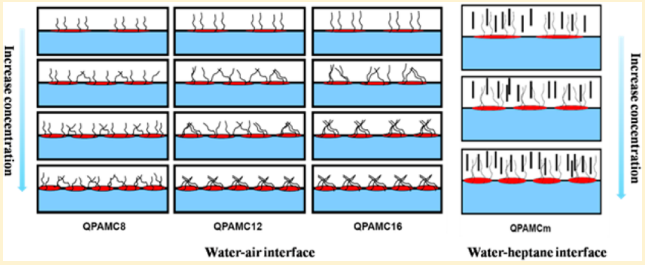

1. INTRODUCTION

Dendrimers reveal unique physical properties due to their monodispersity, such as viscosity, flexibility, and density distribution, which can lead to new materials.[1,2] The multiform modification of end groups, such as the amphiphilic modification, enable the modified dendrimers to have multifarious functions and envisaged properties.[3] Research indicates that tailor-made dendrimers show interesting self-assembly properties when strong dispersive, polar, or hydrogen bonding intermolecular forces are present.[4,5] Amphiphilic dendrimers containing both hydrophilic and hydrophobic segments within the same macromolecule are particularly useful for investigating their surface and interfacial properties.[6] However, little information is available at present on ordering of amphiphilic dendrimers at the interface especially at liquid−liquid interface.

The response of a film of molecules at an interface to expansion and compression is a key factor determining the ease of formation and stability of a multitude of colloidal systems such as emulsions and foams.[7,8] The properties of the interfacial film are governed by the composition and structure of the adsorbed material.[9] Furthermore, the interfacial rheological properties are the main characteristics of the dynamic properties of a film. The study of interfacial dilational properties is useful for better understanding the microcosmic properties of an interfacial film and has been proved to be a powerful technique for probing the interfacial adsorption behaviors.[10] The examination of the adsorptive behaviors of surfactants at the interface is regarded as one of the effective methods for comprehending the relation between their surface-active properties and their molecular structure.[11] Experimental information on the structure and properties of adsorbed conventional surfactants and polymers layers has been comprehensive over the past decade.[12−15] Recently, a great deal of investigations of the interfacial rheology properties of mixed surfactant systems[16,17] and polymer nanocomposites with inorganic nanoparticles[18,19] have been carried out. Although several studies have focused on certain properties of amphiphilic dendrimers, little attention has been paid to the dilational surface viscoelasticity of the amphiphilic dendrimer systems that can provide unique insight into their chemical and

Received: June 8, 2012
Revised: September 30, 2012
Published: October 2, 2012

physical properties.[20] In earlier work we synthesized and studied the aggregation behaviors of nonionic amphiphilic dendrimers modified by PPO−PEO based on PAMAM dendrimers.[21,22] Focusing on the relationship between the structure of modified dendrimers and properties, a series of ionic amphiphilic dendrimers based on generations 1 PAMAM dendrimers modified with different long hydrophobic chains $QPAMC_8$, $QPAMC_{12}$, and $QPAMC_{16}$ were synthesized. To detect the nature of adsorption films formed by these specific molecules, the dilational viscoelastic properties at the water−air and water−*n*-heptane interfaces have been investigated by a drop shape analysis method at low frequency (0.005−0.1 Hz), which is useful for understanding the influence of hydrophilic poly(amidoamine) core or number of hydrophobic hydrocarbon on the interfacial behaviors and the basic intermolecular mechanisms responsible for a given surface rheological characteristic. Hence, these systems should be helpful to understand the interface behaviors of modified PAMAMs, as well as serve model for more complex systems.

2. EXPERIMENTAL SECTION

Materials. The synthesis materials methylacrylate and ethylenediamine were purchased from Beijing Chemical Co and *N*,*N*-dimethyloctylamine, *N*,*N*-dimethyl-decanamide, *N*,*N*-dimethylhexadecylamine were from Aladdin. All of the organic solvents were dried and distilled. Ultrapure water (resistivity >18.2 MΩ·cm) was used in all experiments and measurements of the water surface tension were 72.6 ± 0.1 mN/m. The pH values of all solutions varied from 6.92 to 7.84.

Synthesis. The functionlization of dendrimers in a facile two-step reaction using PAMAM dendrimer as starting material.[23] The products were characterized by ^{1}H NMR, MS−ESI and elemental analysis, and the synthesis pathway together with the data are presented in the Surporting Information.

Surface Dilational Rheological Measurement. The dilational rheological measurements were performed with use of a bubble profile tensiometer (Tracker, IT Concept, France).[10,24] A bubble created by injecting air or n-heptane inside the solution by an inverted needle. Images of the bubble profile were captured, digitized, and analyzed by the Laplace equation to determine surface tension. Then the viscoelastic modulus can be obtained from the change of the surface tension. The bubble in its equilibrium state was expanded and compressed sinusoidally with a small amplitude ($\Delta A/A$, 10%) in a frequency range from 0.005 to 0.1 Hz. The rheological parameters, dilational modulus, phase angle, elasticity, and viscosity, of the interfacial layer are obtained from a Fourier analysis of the measured signals.

Because the theoretical background of interfacial dilational rheology has been reviewed in detail by numerous literatures,[25−28] it will be introduced briefly in this article.

The interfacial dilational modulus (ε) is defined as the ratio between the change in interfacial tension (γ) and relative interfacial area (A):

$$\varepsilon = \frac{d\gamma}{d \ln A}$$

Dilational modulus can also be expressed as the summation of real part (elasticity, ε_d) and imaginary part (viscosity component, ε_η):

$$\varepsilon = \varepsilon_d + i\omega\eta_d(\varepsilon_\eta)$$

The phase angle θ describing the phase difference between dynamic interfacial tension variation and interfacial area variation, the relation among ε_d, ε_η, and θ follows:

$$\tan\theta = \frac{\varepsilon_\eta}{\varepsilon_d}$$

Interfacial Tension Relaxation Measurements. When the equilibrium monolayer is disturbed by a small but fast area expansion or compression, an interfacial tension jump will occur and then the interfacial tension will decay to the equilibrium again. The decay curve can be expressed by the summation of a number of exponential functions:

$$\Delta\gamma = \sum_{i=1}^{n} \Delta\gamma_i \exp(-\tau_i t) = \sum_{i=1}^{n} \Delta\gamma_i \exp(-t/T_i)$$

where τ_i and T_i are the characteristic frequency and period of the *i*th process respectively; $\Delta\gamma_i$ is the fractional contribution that relaxation process makes to restore the equilibrium; n is the total number of the relaxation processes.

In this article, the film was expanded about 10% in area by a sudden expand in 1 s after interfacial equilibrium.

Dynamic Light Scattering (DLS). Measurements were carried out using an LLS spectrometer (ALV/SP−125) with a multi−τ digital time correlater (ALV−5000). Light of λ = 632.8 nm from a solid-state He−Ne laser (22 mW) was used as the incident beam. The measurements were conducted at a scattering angle of 90°. All of the solutions were filtered through a 0.45 μm membrane filter of hydrophilic PVDF before the measurements. The correlation function was analyzed from the scattering data via the CONTIN method to obtain the distribution of diffusion coefficients (D) of the solutes. The apparent hydrodynamic radius R_h was deduced from D by the Stokes−Einstein equation $R_h = K_BT/(6\pi\eta D)$ for spherical particles, where K_B represents the Boltzmann constant, T is the absolute temperature, and η is the solvent viscosity. The measurements were performed at 25.0 (±0.1 °C).

3. RESULTS AND DISCUSSION

3.1. Surface Properties of $QPAMC_m$. The results of dynamic surface/interfacial tension at two different interfaces showed that final equilibrium state needed long time to reach (greater than 10^4 s) especially for $QPAMC_8$ and $QPAMC_{12}$ (Surpporting Information). According to the static surface tension versus log of the bulk concentration for $QPAMC_m$ (Figure 1), the minimum average surface area/surfactant molecule (A_{min}) is obtained from the saturated adsorption by

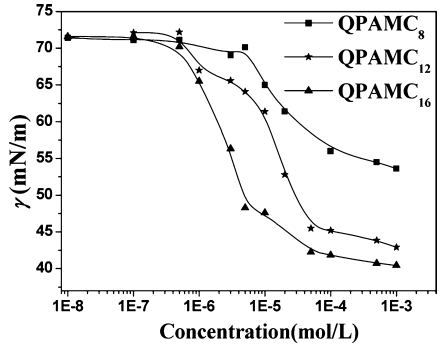

Figure 1. Plot of static surface tension versus log of the bulk concentration for $QPAMC_m$ at 30 °C.

dx.doi.org/10.1021/jp305619n | J. Phys. Chem. B 2012, 116, 12760−12768

Table 1. The CMC, A_{min}, and γ_{cmc} radii of QPAMC$_m$ at 30 °C

sample	CMC (mol/L)	γ_{cmc} (mN/m)	Γ_{min} (μmol/m^2)	A_{min} (Å^2)	saturated adsorbed radius (Å)	theoretical alkyl chain length (Å)
QPAMC$_8$	8×10^{-5}	55.7	0.14	205	8.08	10.16
QPAMC$_{12}$	5×10^{-5}	45.6	0.75	222	8.41	15.24
QPAMC$_{16}$	6.3×10^{-6}	42.2	0.59	280	9.44	20.32

$A_{min} = (N_A\Gamma_{min})^{-1}$, where N_A is the Avogadro constant, $\Gamma = -(1/(2.303nRT))(d\gamma/d\ln C)_T$, Γ is the adsorption amount in μmol/m^2, T is the absolute temperature, R = 8.314 J mol m^{-1} K^{-1}, and $d\gamma/d(\ln C)$ is the maximal slope in each case. For an ionic dendrimer surfactant, n = 4 is taken.[29] The cmc, γ_{cmc}, Γ, and A_{min} of QPAMC$_m$ are listed in Table 1. It is also interesting to point out that with the chain length increase from 8 to 16, A_{min} values augment slightly and the cmc values vary little although the hydrocarbon chain length changes in a wide range.

For conventional linear surfactants, A_{min} decreases obviously when the alkyl chain carbon number increases as a result of the enhancement of hydrophobic nature. In the case of oligomeric surfactants, the A_{min} decreases significantly in going from the monomer to the dimer but varies little.[30] The attractive and repulsive interactions of the surfactant molecules and the conformational entropy of the spacer chain are dominant factors in determining this dependence specific area of dimers on the spacer at the air/water interface by calculating the spacer length corresponds to the maximal specific area of dimers.[31] Saville et al. showed that polyether dendrimers in the layer next to the water interface were ellipsoidal in structure due to compression and contained a volume fraction of about 25% of the substrate water, and the molecules in the layer next to air were spherical with a diameter of 21 Å containing no water, the limiting area of 57 Å^2 for the first generation.[32]

Taking PAMAM dendrimer as the headgroup for QPAMC$_m$, which was considered as a circle model, the calculated area is 1227 Å^2 with a radius of 19.77 Å when fully extended as shown in Figure 2. The A_{min} and saturated adsorbed radii of the three

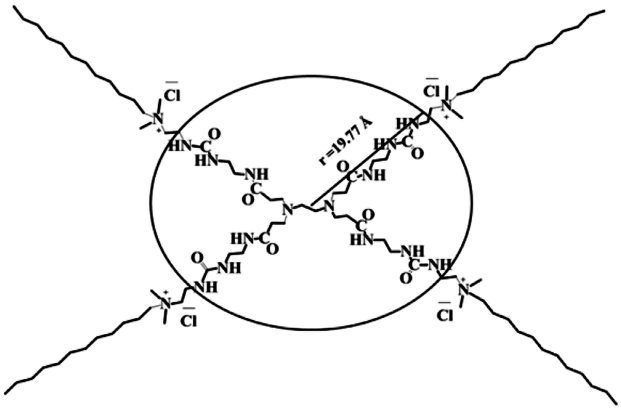

Figure 2. The model of QPAMC$_m$ fully extended.

molecules are smaller than the theoretical values indicating that the molecules could not roll out at the interface. By comparison of the saturated adsorbed radius and theoretical alkyl chain length with theoretical headgroup radius, the data suggest that the intramolecular interaction of alkyl chains becomes stronger with augment of the concentration up to saturated adsorption. For QPAMC$_8$ system, however, the intramolecular interaction of alkyl chains hardly occurs because the alkyl chains are not long enough to overlap across the big headgroup. Therefore, the increasing A_{min} values for QPAMC$_m$ compounds with growing alkyl chain length may be relevant to the little enhancement of hydrophobic nature and the increase of molecular size.[33]

3.2. Dilational Properties of QPAMC$_m$ at the Water–Air Interface. *3.2.a. Influence of Oscillating Frequency on the Dilational Properties of QPAMC$_m$ at the Water–Air Interface.* The influence of oscillating frequency on the dilational modulus (a_1, a_2, and a_3) and phase angle (b_1, b_2, and b_3) at the water–air interface is summarized in Figure 3. For the QPAMC$_m$, the dilational modulus and phase angle increase and decrease monotonically respectively at all experimental bulk concentration.

The frequency dependence of the viscoelasticity provides information about the kinetics of the relaxation processes occurring in the interfacial layer. At lower oscillating frequency, surfactant molecules have enough time to diminish the interfacial tension gradient resulting from the deformation of interface. As the oscillating frequency increases, the restoration of interfacial tension becomes slower as compared with the quick change of interface area leading to a higher interfacial tension gradient. Therefore, dilational modulus increases with increasing oscillating frequency.[34] At low surface coverages, the molecular exchange between bulk and interface is weak when the interface area changes and, therefore, the response of the interface is predominantly elastic in nature and is characterized by low values of the phase angle. The response of the adsorbed layer acquires a viscoelastic character due to transport of surfactant molecules from the bulk to the interface as the concentration increases. This transport mechanism, indicating the presence of a soluble monolayer, reduces the modulus of the adsorbed layers and, eventually, the rheological response of the interface is characterized by low values of the storage modulus and a large phase angle.[35]

The curves of log $|\varepsilon|$ − log ω are quasi-linear for the solutions of QPAMC$_m$, which indicate that the characteristic frequency of the relaxation process at the interfacial layer could be higher than the highest oscillating frequency used in this experiment (0.1 Hz). According to references, the slope ranges of log $|\varepsilon|$ − log ω curves were different if there were different relaxation processes in the system.[36,37] As shown in Figure 4, in the range of experimental frequency, it demonstrates that for QPAMC$_m$ the K values increase with augment of bulk concentration due to the enhanced fast relaxation process, which is accordance with the results obtained above. The tendency of increasing alkyl chain length with bulk concentration indicates that the molecular exchange of QPAMC$_8$ between bulk and interface seems to be weaker than QPAMC$_{12}$ or QPAMC$_{16}$, and the QPAMC$_8$ adsorption film shows the most elastic nature.

3.2.b. Influence of Bulk Concentration on the Dilational Properties of QPAMC$_m$ at the Water–Air Interface. The effect of bulk concentration on the dilational modulus is complex. Generally speaking, the increase of surfactant concentration has two different effects. On the one hand, the molecular exchange between bulk and interface increases, which decreases the interfacial tension gradients and induces a decrease in dilational modulus. On the other hand, the increase of interfacial

dx.doi.org/10.1021/jp305619n | J. Phys. Chem. B 2012, 116, 12760–12768

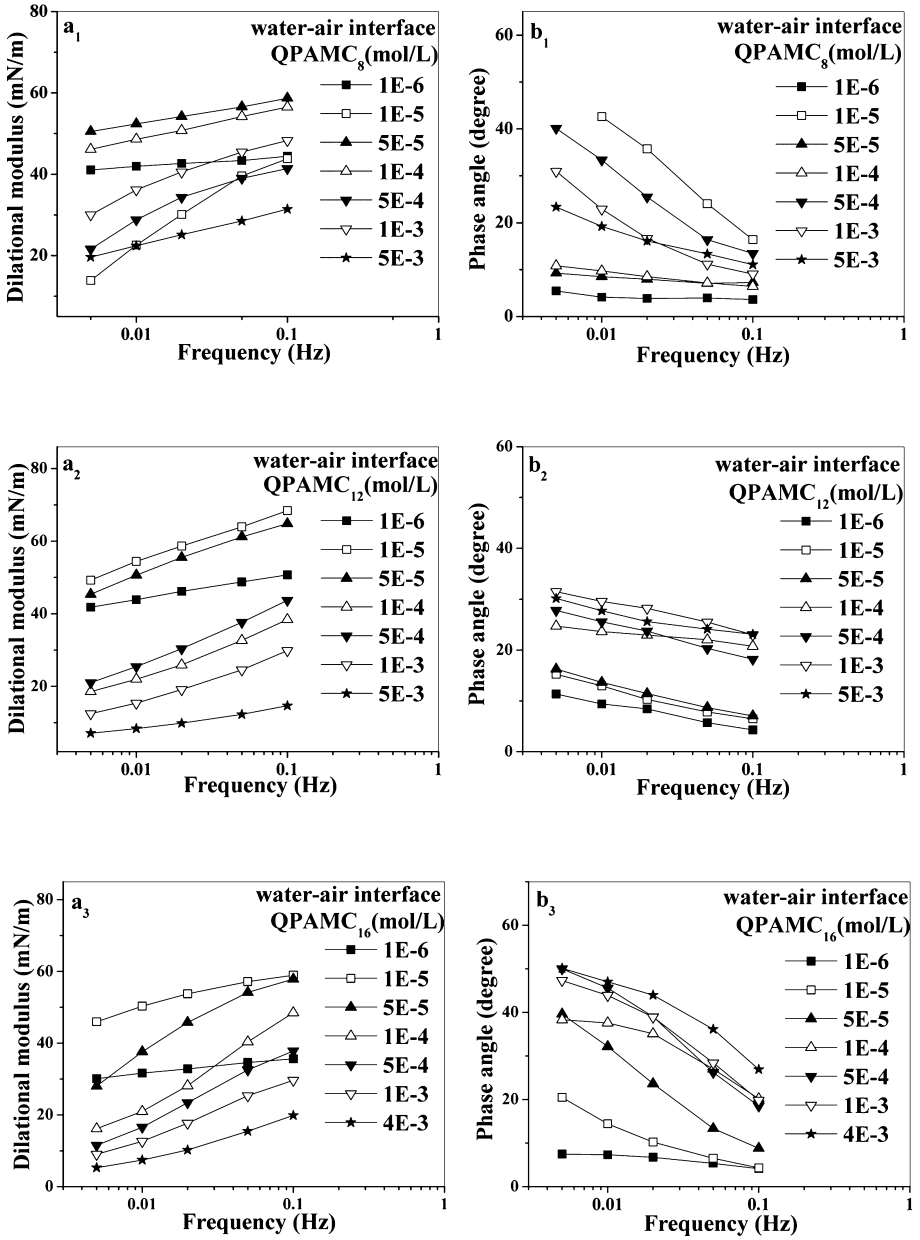

Figure 3. Influence of oscillating frequency on the dilational modulus (a) and phase angle, (b) of $QPAMC_m$ at the water−air interface.

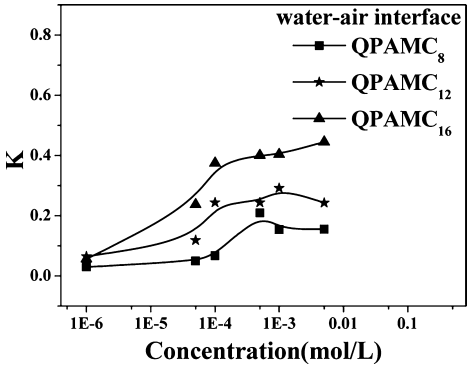

Figure 4. Influence of bulk concentration on the slope of cures of log $|\varepsilon|$ − log ω (K) of $QPAMC_m$ at the water−air interface.

concentration would cause stronger intermolecular interaction and results in increasing of dilational modulus.[38,39] As we know, the dilational modulus increases with the hydrophobic chain length due to the enhancement of hydrophobic interaction and the decreased molecule exchange. And, furthermore, the positions of hydrophobic chains have influence on the dilational modulus.

Figure 5 shows the variations of dilational modulus and phase angle versus bulk concentration for $QPAMC_{16}$ (a, b) and the comparison of dilational parameters for $QPAMC_m$ at the water−air interface at a fixed oscillating frequency of 0.1 Hz (c, d), respectively. A similar tendency of dilational modulus of $QPAMC_m$ can be observed that a maximum presents in the vicinity of cmc with the increasing concentration at higher frequency (0.1 Hz) and decreased gently after the maxima point, while the phase angle increases monotonously.

For small-molecular surfactants, the dilational modulus augment with increasing the length of the hydrophobic group, and the disparity in modulus is 10 to 30 mN/m or even more when there is three difference of hydrophobic

dx.doi.org/10.1021/jp305619n | J. Phys. Chem. B 2012, 116, 12760−12768

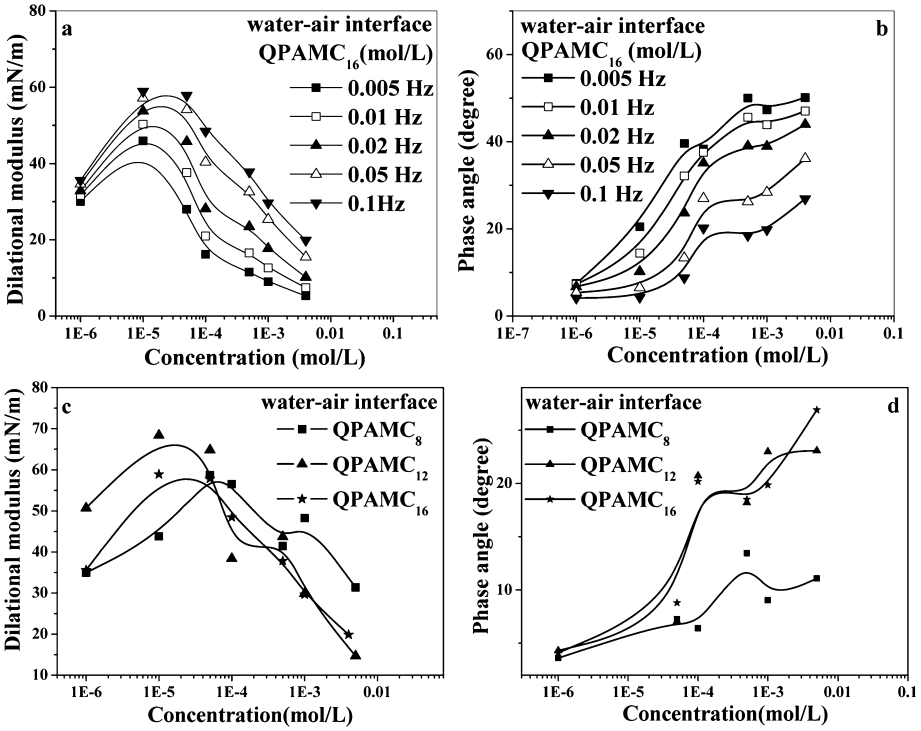

Figure 5. Influence of bulk concentration on the dilational modulus (a) and phase angle, (b) of $QPAMC_{16}$ at the water−air interface and the comparison of the three structures at a fixed oscillating frequency of 0.1 Hz (c, d).

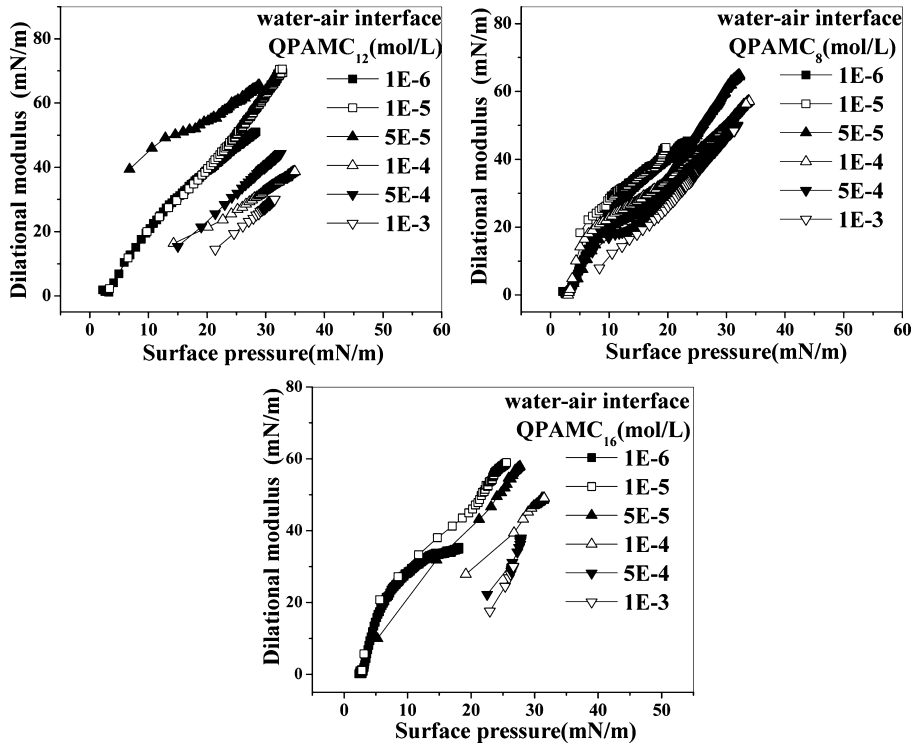

Figure 6. Influence of surface pressure on the dilational modulus of $QPAMC_m$ at the water−air interface.

carbon.[40] However, by comparison the properties of $QPAMC_m$, the maximum values of dilational modulus seem to have no obvious change from $QPAMC_8$ to $QPAMC_{16}$. In general, the diffusion coefficient (D) decreases with an increase of the surfactant concentration.[41] For $QPAMC_{12}$, the value of diffusion coefficient varies from 1×10^{-9} to 1×10^{-10} m^2/s measured by the 2D DOSY PGSE NMR experiments. However, phase angle increases with both the bulk concentration and alkyl chain length, which is similar to the variation of slopes of log $|\varepsilon|$ − log ω curve.

3.2.c. Surface Dilational Modulus As a Function of Surface Pressure for $QPAMC_m$ at the Water−air Interface. It is well known that in some cases the effect of protein concentration and adsorption time on the dilational modulus can be explained

dx.doi.org/10.1021/jp305619n | J. Phys. Chem. B 2012, 116, 12760−12768

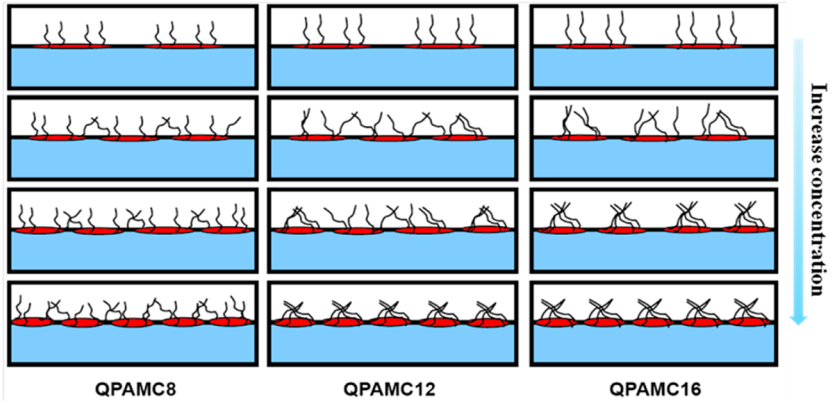

Figure 7. Possible models of adsorbed molecules $QPAMC_m$ at the water−air interface.

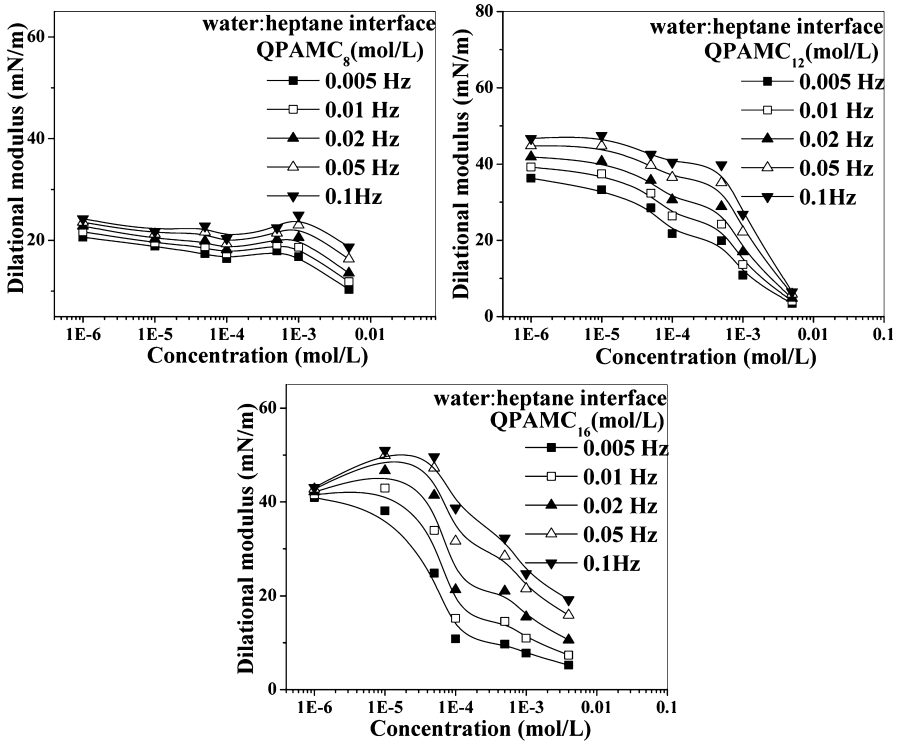

Figure 8. Influence of bulk concentration on the dilational modulus of $QPAMC_m$ at the water−*n*-heptane interface.

quantitatively as an effect of varying molecular adsorption: the measured moduli are in agreement with limiting values up to a certain surface pressure, implying that the surface behaves in a purely elastic manner. Above the value, the curve is split into different branches for the different frequencies specific for visco-elastic behavior,[42] which means that the influence of surface pressure on the dilational modulus reflects the process of diffusion-exchange. It can be seen clearly from Figure 6 that the curves of dilational modulus versus surface pressure for $QPAMC_m$ are quite different. The dilational moduli for $QPAMC_8$ at different adsorption time and at various concentrations coincide on a single modulus vs surface pressure curve, which indicates that the in-surface process dominates the film properties and the diffusion-exchange process can be neglected. However, in the case of long alkyl chains, such as $QPAMC_{12}$ or $QPAMC_{16}$, the diffusion-exchange process dominates the nature of the film when the surface pressure is higher than 20 mN/m.

According to all the experimental data mentioned above, the adsorption characteristic of $QPAMC_m$ can be schematically showed in Figure 7.

It is commonly assumed in the dendrimer literature that flexible hydrophobic end-groups of amphiphilic dendrimers are mainly directed toward one side when confined by a surface or interface.[43] The headgroups of $QPAMC_m$ in the adsorption film are different depending on the surface concentration. At low bulk concentration, the headgroups of $QPAMC_m$ spread completely on the surface, which can be represented by a circular with radius of about 20 Å (Figure 2). With the increasing concentration, the headgroups will partly enter the bulk and show ellipsoidal in structure. The radii of $QPAMC_m$ at the surface are 8.08 Å, 8.41 Å and 9.44 Å for $QPAMC_8$, $QPAMC_{12}$, and $QPAMC_{16}$ respectively when saturated adsorption reaches. The orientation of alkyl chain of $QPAMC_m$ strongly depends on alkyl chain length and occupied surface area of headgroup.

dx.doi.org/10.1021/jp305619n | J. Phys. Chem. B 2012, 116, 12760−12768

In the case of $QPAMC_8$, at low surface concentration, flexible hydrophobic end-groups are mainly directed toward one side when confined by a surface, with no obvious intermolecular action existing between hydrophobic chains. With the increase of surface concentration, the intermolecular hydrophobic interaction of $QPAMC_8$ becomes stronger, enhancing the dilational modulus and elasticity. Whereas with the chain length increase to 12 or 16, the alkyl chains are long enough to interact intramolecularly forming hydrophobic domain (Table 1). Even though at high concentration range, the intermolecular hydrophobic interaction is weaker than $QPAMC_8$. The strong intermolecular interaction between $QPAMC_8$ will slow diffusion-exchange process leading to more elastic nature of adsorption film, as can be seen from dilational experimental results above. However, the intracohesion of alkyl chain results in enhancing diffusion-exchange process. Therefore, the dilational modulus values change little with the increase of alkyl chain length. To test and verify the deduction, dilational properties of $QPAMC_m$ are studied at the water−heptane interface.

3.3. Dilational Properties of $QPAMC_m$ at the Water−Heptane Interface. The dilational properties of $QPAMC_m$ at the water−heptane interface are observed to be similar to that at the water−air interface, such as the influence of oscillating frequency on the dilational modulus and the phase degree, the influence of surface pressure on the dilational modulus. However, there is considerable variability in the tendency of the influence of bulk concentration on the dilational modulus of $QPAMC_m$ at two different interfaces, which is showed as Figure 8. The change of dilational modulus with increasing bulk concentration becomes smooth, especially for $QPAMC_8$. To compare, the concentration dependence of dilational modulus maximum at both water−air and water−heptane interfaces at 0.1 Hz were shown together in Figure 9.

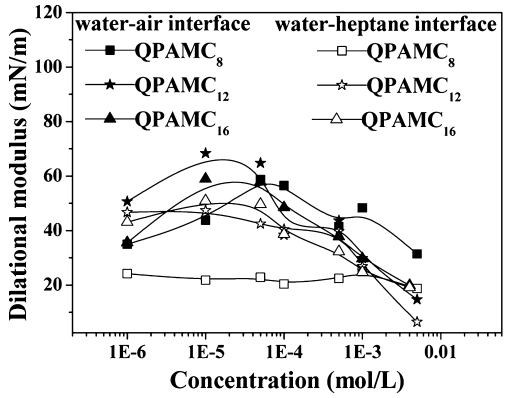

Figure 9. Concentration dependence of dilational modulus for $QPAMC_m$ at frequency of 0.1 Hz.

3.4. Comparison of Dilational Modulus for $QPAMC_m$ between the Water−Air and Water-*n*-Heptane Interface. It can be seen easily from Figure 9 that the modulus values at water−heptane interface are slightly lower than those at water−air interface for $QPAMC_{12}$ and $QPAMC_{16}$. However, it is worth noting that abnormal results for $QPAMC_8$ are observed, in which the dilational modulus decreased sharply, reducing twice as much as the water−air interface. It is also interestingly found that the maximum dilational modulus of $QPAMC_8$ disappeared and no obvious change can be observed with increasing of bulk concentration.

As shown in Figure 10, in the case of the water−oil interface, the oil molecules are inclined to intervene into the surfactant

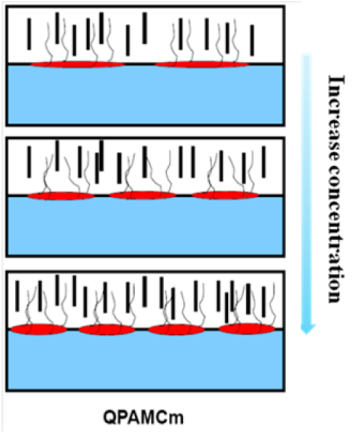

Figure 10. Reasonable model of adsorbed $QPAMC_m$ at the water−heptane interface.

molecules, which results in the decrease of hydrophobic interactions and the dilational modulus decreases sharply. However, heptane molecules will also intervene into the alkyl chains, which will weaken the intracohesion of alkyl chains. As Albertus et al. mentioned,[44] the dendritic poly(amidoamine) part act as a polar headgroup and the alkyl chains are packed together forming a hydrophobic unit, in which case, the headgroup of $QPAMC_m$ is flexible and huge. In the case of $QPAMC_{12}$ or $QPAMC_{16}$, the intramolecular interaction of hydrophobic chains plays a major role when absorbed at the surface to form cohesive conformation. Once the systems are exposed to oil phase, the oil molecules intervene into amphiphilic molecules, and shatter the intermolecular interaction. The counteraction between weakened intermolecular interaction and enhanced molecular size will result in little difference for dilational moduli at the two interfaces.

It is unusual for the tendency of $QPAMC_8$ which is much different from $QPAMC_{12}$ and $QPAMC_{16}$. The C_8 alkyl chains are not long enough to interact together to form hydrophobic domain relative to the big size of headgroup, so the hydrophobic chains of $QPAMC_8$ act in the form of intermolecular and, as a result, the in-surface interaction between alkyl chains plays a crucial role in determining the nature of adsorption film. Because of the intervention of oil molecules, the intermolecular hydrophobic interaction is weakened and the molecular size varies little. As a result, the dilational modulus decreases sharply at water−heptane interface. The dilational modulus varies little with increasing of bulk concentration, which may be a result of the counteraction of weakened hydrophobic interaction and molecule diffusion.

The dilational properties at the water−heptane are in accordance with the mechanism provided in Figure 7. Furthermore, to verify this possible mechanism, relaxation experiments have been employed, and the results will be discussed in the following parts.

3.5. Comparison of Relaxation Processes of $QPAMC_m$ at the Water−Air Interface and Water−Heptane Interface. The mechanism of microscopic relaxation processes can be revealed by the results from the interfacial tension relaxation measurements. One can determine the characteristic relaxation frequency τ_i and contribution of different relaxation processes

dx.doi.org/10.1021/jp305619n | J. Phys. Chem. B 2012, 116, 12760−12768

Table 2. Relaxation Time and Contributions of the Fastest Relaxation Processes

	$QPAMC_8$		$QPAMC_{12}$		$QPAMC_{16}$	
concentration (mol/L)	$\Delta\gamma$ (mN/m)	τ (s)	$\Delta\gamma$ (mN/m)	τ (s)	$\Delta\gamma$ (mN/m)	τ (s)
			Water−air interface			
1×10^{-6}	0.32	316.45	0.62	11.25	0.11	9.33
1×10^{-5}	2.55	5.56	1.87	19.20	0.21	3.50
1×10^{-4}	0.68	13.27	1.46	3.03	1.87	3.52
1×10^{-3}	2.14	20.02	1.99	1.04	0.32	0.27
			Water−heptane interface			
1×10^{-6}	0.28	4.37	0.6	7.17	0.10	14.37
1×10^{-5}	0.30	3.83	1.17	7.46	0.23	6.34
1×10^{-4}	0.26	1.96	1.17	4.34	2.03	4.06
1×10^{-3}	0.67	3.88	1.23	1.26	0.69	2.36

$\Delta\gamma_i$, which are connected with the dynamic aggregation characteristics of molecules and provide the most important information about relaxation processes.

Generally speaking, the theory of Lucassen and van den Tempel[45] is widely used for usual surfactant systems. For $QPAMC_m$, there exists more than one main relaxation processes for complex molecules. Among these processes, the fastest relaxation may be related to the diffusion-exchange process. The characteristic relaxation time and contributions of the fastest relaxation processes for $QPAMC_m$ at different concentrations are listed in Table 2. It can be seen that for the characteristic time of process for $QPAMC_{16}$ are almost the smallest at water−air interface and the largest at water−heptane interface. The characteristic time values of surface are smaller than those of interface. However, the contrary trends can be observed in the case of $QPAMC_8$. The characteristic time of surface process for $QPAMC_8$ is far more than others at low concentration, which means that the fastest process can be neglected. In the case of $QPAMC_{12}$, the variations of characteristic time seem to be similar to $QPAMC_8$ at low bulk concentration and $QPAMC_{16}$ at high bulk concentration respectively.

According to the experimental results of characteristic time, one can conclude that $QPAMC_8$ shows the slowest fast-process at surface, which is believed to be resulted from the intermolecular interaction between alkyl chain. However, $QPAMC_{16}$ shows the slowest fast-process at the interface because the oil molecules can destroy intramolecular cohesion of alkyl chains and enlarge the molecular size. The relaxation data strongly supports our provided mechanism above.

3.6. DLS Measurements of the Size Distributions of $QPAMC_m$ at Various Concentrations. To further understand the unique assignment of $QPAMC_m$ at the interface, the aggregate particle size distributions of $QPAMC_m$ in solutions were also determined with dynamic light scattering (DLS) at rather high concentrations ($>10^{-5}$ M). We focus on the size distribution of around 3 nm, which is a kind of special premicellar aggregates representing the aggregation process.[46] Figure 11 shows the size distributions of $QPAMC_m$ at various concentrations.

At the same concentration range, with increasing of hydrophobic chain length, the size distribution of small aggregates gradually decrease and finally disappear for $QPAMC_{16}$. The phenomena show that strong intramolecular hydrophobic interaction is prone to form large aggregates. However, in the case of $QPAMC_8$, the intermolecular interaction dominates the aggregation behavior, and, consequently, small aggregates may exist before the formation of large aggregates, due to the repulsion among the highly charged particles which hinders the formation of large size of aggregates.[47]

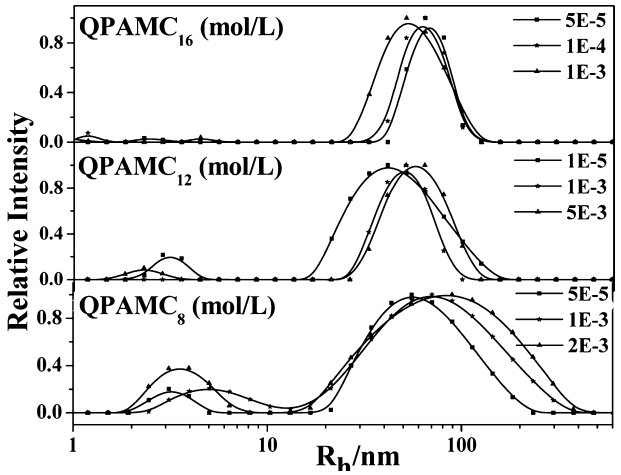

Figure 11. DLS measurements of the size distributions of $QPAMC_m$ at various concentrations at 30 °C.

4. CONCLUSIONS

In summary, amphiphilic dendrimers taking generation 1 PAMAM as the core synthesized by a simple two-step reaction pathway are proposed in this work. The dilational properties are studied as monolayers at the water−air and water−*n*-heptane interfaces with a drop shape analysis method. It is revealed from the experimental results that the hydrophobic tails attached to hydrophilic PAMAM dendrimers are one of the principal factors to control the nature of the interfacial film. The maximum values of dilational modulus vary little from $QPAMC_8$ to $QPAMC_{16}$ and the trends change distinctly at the two different interfaces, which demonstrate that the adsorption behaviors presented reverse the tendency of conventional surfactants. In the case of short hydrophobic chain length such as $QPAMC_8$, the intermolecular hydrophobic interaction is primary, which enhances the dilational modulus and elasticity at the water−air interface. When at the water−heptane interface, the intermolecular hydrophobic interaction is weakened due to intervening of oil molecules, as a result, the dilational modulus decreases sharply. With the chain length increasing to 12 or 16, the alkyl chains become long enough to form cohesive conformation and the intracohesion of alkyl chains results in enhancing the diffusion-exchange process, that is why dilational moduli changing so little. After intervening of oil molecules in

dx.doi.org/10.1021/jp305619n | J. Phys. Chem. B 2012, 116, 12760−12768

the cohesive hydrophobic domain, which impairs the action of intracohesion, the counteraction between weakened intramolecular interaction and enhanced molecular size will result in little difference for dilational moduli at the two interfaces. The results of relaxation experiments indicate that $QPAMC_8$ shows the slowest fast-process at surface and $QPAMC_{16}$ shows the slowest fast-process at interface, which are in agreement with the deduction of intermolecular interaction for short chain length and intracohesion for long alkyl chains. DLS data are consistent with the conclusion mentioned above and support the proposed mechanism simultaneously.

■ ASSOCIATED CONTENT

Supporting Information

$QPAMC_m$ synthesis, characterization data by ^1H NMR, mass spectrum, elemental analysis and dynamic surface/interfacial tension. This material is available free of charge via the Internet at http://pubs.acs.org.

■ AUTHOR INFORMATION

Corresponding Author

*E-mail: jbwang@iccas.ac.cn, phone: 86-10-62523395, fax: 86-10-62523395.

Notes

The authors declare no competing financial interest.

■ ACKNOWLEDGMENTS

We are grateful to Sui Zhao group of Technical Institute of Physics and Chemistry, Chinese Academy of Sciences, for partial experimental support of these studies. The authors are thankful for financial support from the Important National Science and Technology Specific Project (2011ZX05024-004-03) of China and the Knowledge Innovation Project of Chinese Academy of Sciences (KJCX-1-YW-21-03).

■ REFERENCES

(1) Scherrenberg, R.; Coussens, B.; Vliet, Paul van; Edouard, G.; Brackman, J.; de Brabander, Ellen.; Mortensen, K. *Macromolecules* **1998**, *31*, 456−461.
(2) Bosman, A. W.; Janssen, H. M.; Meijer, E. W. *Chem. Rev.* **1999**, *99*, 1665−1688.
(3) Vogtle, F.; Gestermann, S.; Hesse, R. *Prog. Polym. Sci.* **2000**, *25*, 987−1041.
(4) Yoon, H. C.; Hong, M. Y.; Kim, H. S. *Anal. Chem.* **2000**, *72*, 4420−4427.
(5) Albertazzi, L.; Storti, B.; Marchetti, L.; Beltram, F. *J. Am. Chem. Soc.* **2010**, *132*, 18158−18167.
(6) Tully, D. C.; Frechet, J. M. J. *Chem. Commun.* **2001**, 1229−1239.
(7) Sun, H. Q.; Zhang, L.; Li, Z. Q.; Zhang, L.; Luo, L.; Zhao, S. *Soft Matter* **2011**, *7*, 7601−7611.
(8) Bomqvistt, B. R.; Warnheim, T.; Claesson, P. M. *Langmuir* **2005**, *21*, 6373−6384.
(9) Gomez, J. M. A.; Patino, J. M. R. *J. Phys. Chem. C* **2007**, *111*, 4790−4799.
(10) Huang, Y. P.; Zhang, L.; Luo, L.; Zhao, S.; Yu, J. Y. *J. Phys. Chem. B* **2007**, *111*, 5640−5647.
(11) Fuhrhop, J. H.; Liman, U. *J. Am. Chem. Soc.* **1984**, *106*, 4643−4644.
(12) Miller, R.; Leser, M. E.; Michel, M.; Fainerman, V. B. *J. Phys. Chem. B* **2005**, *109*, 13327−13331.
(13) Klebanau, A.; Kliabanova, N.; Ortega, F.; Monroy, F.; Rubio, R. G.; Starov, V. *J. Phys. Chem. B* **2005**, *109*, 18316−18323.
(14) Jain, N. J.; Albouy, P. A.; Langevin, D. *Langmuir* **2003**, *19*, 8371−8379.
(15) Feng, J.; Liu, X. P.; Zhang, L.; Zhao, S.; Yu, J. Y. *Langmuir* **2010**, *26*, 11907−11914.
(16) Noskov, B. A.; Loglio, G.; Miller, R. *Adv. Colloid Interface Sci.* **2011**, *168*, 179−197.
(17) Latnikova, A. V.; Lin, S. Y.; Loglio, G.; Miller, R.; Noskov, B. A. *J. Phys. Chem. C* **2008**, *112*, 6126−6131.
(18) Whitby, C. P.; Fornasiero, D.; Ralston, J.; Liggieri, L.; Ravera, F. *J. Phys. Chem. C* **2012**, *116*, 3050−3058.
(19) Geiser, V. R.; Leterrier, Y.; Månson, J.A. E. *Macromolecules* **2010**, *43*, 7705−7712.
(20) Yoshimura, T.; Fukai, J.; Mizutani, H.; Esumi, K. *J. Colloid Interface Sci.* **2002**, *255*, 428−431.
(21) Yang, H.; Hu, C. C.; Wu, X.; Chen, H. B.; Wang, J. B. *Supramol. Chem.* **2010**, *22*, 477−482.
(22) Zhang, W.; Dong, G. J.; Yang, H.; Sun, J. H.; Zhou, J. Z.; Wang, J. B. *Colloids Surf. A* **2009**, *348*, 45−48.
(23) Chen, C. Z. S.; Beck-Tan, N. C.; Dhurjati, P.; van Dyk, T. K.; LaRossa, R. A.; Cooper, S. L *Biomacromolecules* **2000**, *1*, 473−480.
(24) Ravera, F.; Ferrari, M.; Santini, E.; Liggieri, L. *Adv. Colloid Interface Sci.* **2005**, *117*, 75−100.
(25) Li, Y. M.; Xu, G. Y.; Xin, X.; Cao, X. R.; Wu, D. *Carbohydr. Polym.* **2008**, *72*, 211−221.
(26) Noskov, B. A.; Akentiev, A. V.; Bilibin, A. Y.; Zorin, I. M.; Miller, R. *Adv. Colloid Interface Sci.* **2003**, *104*, 245−271.
(27) Noskov, B. A.; Loglio, G.; Miller, R. *J. Phys. Chem. B* **2004**, *108*, 18615−18622.
(28) Noskov, B. A.; Latnikova, A. V.; Lin, S. Y.; Loglio, G.; Miller, R. *J. Phys. Chem. B* **2007**, *111*, 16895−16901.
(29) Jurasin, D.; Habus, I.; Filipovic-Vincekovic, N. *Colloids Surf. A* **2010**, *368*, 119−128.
(30) In, M.; Bec, V.; Aguerre-Chariol, O.; Zana, R. *Langmuir* **2000**, *16*, 141−148.
(31) Diamant, H.; Andelman, D. *Langmuir* **1994**, *10*, 2910−2916.
(32) Saville, P. M.; Reynolds, P. A.; White, J. W. *J. Phys. Chem.* **1995**, *99*, 8283−8289.
(33) Mulqueen, M.; Blankschtein, D. *Langmuir* **1999**, *15*, 8832−8848.
(34) Wustneck, R.; Prescher, D.; Katholy, S.; Knochenhauer, G.; Brehmer, L. *Colloids Surf. A* **2000**, *175*, 83−92.
(35) Rao, A.; Kim, Y.; Kausch, C. M.; Thomas, R. R. *Langmuir* **2006**, *22*, 7964−7968.
(36) Vanden Tempel, M.; Lucassen-Reynders, E. H. *Adv. Colloid Interface Sci.* **1983**, 281−301.
(37) Wang, H. R.; Gong, Y.; Lu, W. C.; Chen, B. L. *Appl. Surf. Sci.* **2008**, *254*, 3380−3384.
(38) Maldonado-Valderrama, J.; Fainerman, V. B.; Galvez-Ruiz, M. J.; Martin-Rodriguez, A.; Cabrerizo-Vilchez, M. A.; Miller, R. *J. Phys. Chem. B* **2005**, *109*, 17608−17616.
(39) Ma, B. D.; Zhang, L.; Gao, B. Y.; Zhao, S.; Yu, J. Y. *Colloid Polym. Sci.* **2011**, *289*, 911−918.
(40) Zhang, L.; Wang, X. C.; Gong, Q. T.; Luo, L.; Zhao, S.; Yu, J. Y. *J. Colloid Interface Sci.* **2008**, *327*, 451−458.
(41) Lee, K.; Shim, S. E.; Lee, B. H.; Hong, S. U.; Choe, S. *J. Polym. Sci., Part B: Polym. Phys.* **2004**, *42*, 1114−1126.
(42) Bos, M. A.; van Vliet, T. *Adv. Colloid Interface Sci.* **2001**, *91*, 437−471.
(43) Yoshimura, T.; Yoshida, H.; Ohno, A.; Esumi, K. *J. Colloid Interface Sci.* **2003**, *267*, 167−172.
(44) Albertus, P. H. J. Schenning.; et al. *J. Am. Chem. Soc.* **1998**, *120*, 8199−8208.
(45) Lucassen, J; van den Tempel, M. *Chem. Eng. Sci.* **1972**, *27*, 1283−1291.
(46) Yoshimura, T.; Esumi, K. *Langmuir* **2003**, *19*, 3535−3538.
(47) In, M.; Aguerre-Chariol, O.; Zana, R. *J. Phys. Chem. B* **1999**, *103*, 7747−7750.